CrossMark

Electrons Trapped in Solid Neon–Hydrogen Mixtures Below 1 K

S. Sheludiakov[1,2] · J. Ahokas[1] · J. Järvinen[1] · L. Lehtonen[1] · S. Vasiliev[1] ·
Yu. A. Dmitriev[3] · D. M. Lee[2] · V. V. Khmelenko[2]

Abstract

We report on an electron spin resonance study of electrons stabilized in solid films of neon–hydrogen mixtures. We found that these films are highly porous and may absorb large amount of liquid helium. We observed that free electrons can be stabilized in two different positions: in a pure neon environment and in H_2 clusters formed in the pores of solid neon. It turned out that the presence of the superfluid helium film suppresses the escape of the trapped electrons via diffusion through the pores and stimulates their accumulation in the H_2 clusters even in Ne samples of the best available purity. We propose several possible explanations for this behavior.

Keywords Matrix stabilization · Free electrons · Electron spin resonance

1 Introduction

Matrix isolation is one of the most widespread and convenient techniques for stabilizing and investigating highly reactive species and radicals [1–3]. Being introduced into an inert solid matrix, these species become immobilized and remain stable at low enough temperatures where their diffusion is suppressed. A weak van-der-Waals inter-

✉ S. Vasiliev
  servas@utu.fi

  S. Sheludiakov
  seshel@physics.tamu.edu

[1] Department of Physics and Astronomy, University of Turku, 20014 Turku, Finland

[2] Department of Physics and Astronomy, Institute for Quantum Science and Engineering, Texas A&M University, College Station, TX 77843, USA

[3] Ioffe Physical-Technical Institute, 26 Politekhnicheskaya, St. Petersburg, Russian Federation 194021

action, low atomic polarizability and a large bandgap make solid neon a particularly suitable medium for conducting optical and electron spin resonance studies of such transient species. In contrast to atomic hydrogen, the smallest among the metastable radicals, which may occupy two different positions in a solid neon lattice [4–6], observation of electrons in a Ne matrix is far more difficult due to the large -1.3 eV negative electron affinity of neon atoms [7]. However, exposure of solid neon samples to an electron beam is accompanied by a large yield of secondary electrons, which is $\simeq 60$ for each incident 1–3 keV primary electron [8]. The small atomic polarizability also makes solid neon films a promising substrate for stabilization of a high-density 2D electron gas [9]. However, only a partial wetting of surfaces below its triple point makes solid neon films highly disordered and porous [10,11].

The pairwise Ne–Ne interaction is nearly identical to that between Ne atoms and H_2 molecules. This allows considering Ne and H_2 solutions to be isotopic mixtures with an astonishingly large mass difference. As a result, the equilibrium solubility of H_2 in solid neon at temperatures of order 1 K is limited to a fraction of percent while both Ne and H_2 in solid non-equilibrium mixtures may form fcc and hcp structures depending on the H_2 admixture [12,13].
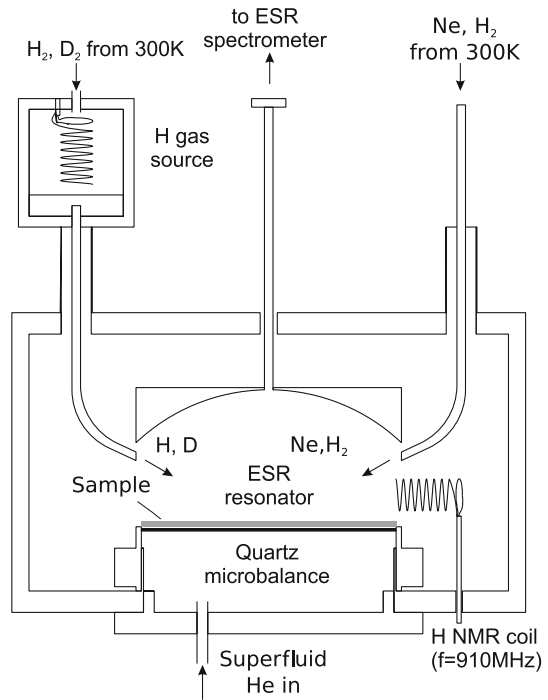
In our recent study [6], we found that the solid neon with small (well below 6%) admixtures of hydrogen forms a highly porous solid with small clusters of pure H_2 embedded inside the pores. We observed an exceptionally high recombination rate of H atoms in such H_2 clusters upon raising the temperature to 0.3–0.6 K, which could be explained by a solid-liquid transition in the clusters. The possibility of such a transition was predicted earlier for solid H_2 in a restricted geometry [14]. These results motivated us to explore other methods to study the properties of such hydrogen clusters formed inside solid Ne.

In addition to the ESR signals of atomic hydrogen in the solid neon–hydrogen mixtures, we also detected two singlet lines from free electrons trapped inside the films. In the present work, these electrons serve as an additional probe of the sample porosity and the local distribution of molecular hydrogen in a solid neon matrix. We present here a detailed study of the behavior of electrons trapped in solid Ne matrices containing small admixtures of H_2. We found that depending on a H_2 admixture, electrons may be trapped in two locations inside the neon matrix. In one such location, the electrons are surrounded mostly by pure neon and are probably trapped in the neon lattice near the surface of the pores. The electrons of the second type are located in the bulk of hydrogen clusters inside the pores. We found that condensing superfluid helium into the pores blocks the diffusion of these electrons from the pores and leads to a substantial growth of their concentration.

2 Experimental Setup

The experimental setup is based on an Oxford 2000 dilution refrigerator which accommodates a sample cell (Fig. 1) and a 128 GHz ESR spectrometer [15]. The sample cell is placed in the center of a 4.6 T superconducting magnet and is attached to the mixing chamber of the dilution refrigerator to provide cooling. The main investigation tool in our experiments is a 128 GHz super-heterodyne ESR spectrometer which enables

Fig. 1 The sample cell schematic

simultaneous measurement of both the absorption and dispersion parts of the mm-wave susceptibility [16]. We will present only the absorption part throughout this article. The ESR resonator in the sample cell has an open Fabry–Perot design which also allows installation of the capillaries for condensing Ne:H_2 mixtures and an auxiliary rf resonator (HNMR in Fig. 1). The bottom ESR resonator mirror also serves as the top electrode of a quartz microbalance (QM) which makes it possible to measure the ESR signals of species with unpaired electron spins and accurately determine the film thickness. The top electrode of the quartz microbalance is left floating which provides the possibility of applying an electric potential to the film substrate. The top ESR resonator mirror has a spherical shape and is made of oxygen-free polycrystalline copper.

We used neon gas of 99.99% purity with a 100 ppm natural H_2 admixture. The Ne:H_2 mixtures were prepared at room temperature and the solid neon–hydrogen films were deposited onto the top electrode of the QM directly from a gas-handling system with a typical rate of 0.1 monolayers/s, resulting in the final thickness of 2.5 μm. The substrate temperature during the Ne:H_2 film deposition was stabilized at temperature 0.7–1.3 K which was slightly different during preparation of different samples. Prior to that, a small amount of He gas ($\sim$ mmol) was condensed into a chamber below the quartz microbalance in order to form a saturated helium film there. The superfluid film flushes the bottom QM surface and removes heat dissipated during sample deposition.

The present sample cell was previously used for studies of solid tritium films [17] and, as a result, a certain number of tritium atoms and molecules diffused into the

ESR mirrors and the copper walls of the sample cell. These tritium impurities serve as a constant source of 5.7 keV electrons resulting from its β-decay. The amount of trapped tritium and the flux of electrons remains nearly unchanged after warming up the sample cell to room temperature and starting a new experimental run. These electrons are continuously released from the sample cell walls and lead to an effective dissociation of H_2 molecules in Ne:H_2 solid samples, so that discernible signals of H atoms can be observed after a few hours of sample storage even in the samples with the smallest admixture of H_2 (100 ppm). While moving inside the H_2–Ne solid, the electrons slow down and a fraction of them get trapped in the matrix.

Along with the H atoms trapped inside solid Ne:H_2 films, we were also able to create H and D atoms in the gas phase. The reference ESR lines of H and D atoms in the gas phase were employed for determining the spectroscopic parameters of the species trapped in the Ne:H_2 samples.

3 Experimental Results

3.1 Samples and ESR Spectra

In order to investigate the influence of H_2 admixture on the ESR spectra of trapped electrons, we studied several samples with different Ne:H_2 compositions: a "pure" Ne Sample 1 ([H_2]=100 ppm) where we did not add H_2 intentionally, Ne:0.2% H_2 (Sample 2), Ne:1% H_2 (Sample 3), Ne:3% H_2 (Sample 4), Ne:6% H_2 (Sample 5) and a pure H_2 sample (Sample 6).

All samples studied were stored at $T \simeq 0.09$ K, the lowest temperature attained in this experimental run, for a time period of several days in order to achieve strong enough ESR signals from H atoms and electrons (Fig. 2). The H atom lines had a complex shape resulted from their stabilization in different lattice sites: trapping in substitutional sites of a pure H_2 environment (Component 1) and in substitutional positions of solid Ne (Components 2 and 3). The fitting procedure and detailed explanation of different trapping sites of H atoms in Ne:H_2 solid mixtures is presented in Ref. [6].

In addition to the doublets of trapped H atoms, we also observed distinct lines in the center of the ESR spectra. Depending on H_2 content, we observed either one or two ESR lines, one narrow with the width of 0.7 G and a much broader line with the width of 2.1–3 G, respectively, shifted from the narrow line by 2–6 G (Fig. 3). The electronic g-factors of both lines were determined by comparing their positions with the position of the reference ESR line of gas-phase atomic deuterium produced by running the rf discharge in the gas-source (Fig. 1). The value $g = 2.00234(1)$ extracted for the narrow line well matched that of electrons trapped in pure H_2 observed in the sample 6 and our previous work [18]. This is slightly, by $\sim 1 \times 10^{-5}$, larger than the g-factor of the free electron. The narrow component had a Gaussian line shape with the width equal to that of the line of electrons in pure H_2 matrix. Based on these observations, we associated the observed lines with electrons trapped in different positions of solid Ne:H_2 samples: in a pure Ne environment (broad line) and in the H_2 clusters formed in solid Ne (narrow line). We label these lines as e-Ne line and e-H_2 line, respectively.
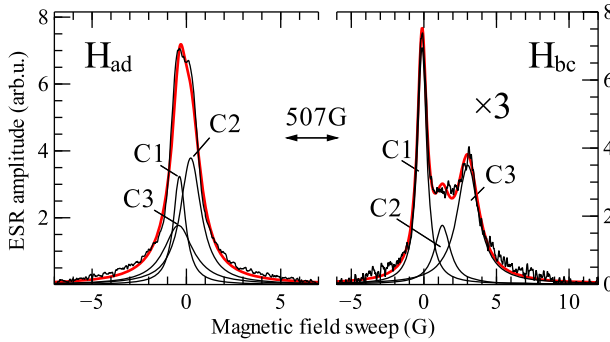
Fig. 2 ESR spectra of H atoms acquired during storage of Sample 3 (Ne:1% H_2) Low-field a–d line is shown on the left, high-field b–c line is shown on the right. Both lines are fitted by three Lorentzian components, labeled C_1–C_3 (Color figure online)

The electron lines typically increased during the first 1–2 days of storage with their growth stalling afterward, while the ESR lines of H atoms continued to increase further. Decay of tritium atoms embedded in the sample cell walls and ESR resonator mirrors provides a constant flux of electrons on the time scale of the experiment. Therefore, it might be suggested that there exists a mechanism responsible for the electron disappearance which compensate for the growth of both (e-H_2 and e-Ne) lines.

The e-Ne line was observed in Samples 1–3 with small H_2 admixtures in Ne (100 ppm, 0.2% and 1% H_2, respectively). In contrast to those situations, the e-H_2 appeared in samples with the larger H_2 contents of 1, 3, 6 % and the pure H_2 sample (Samples 3–6). We observed both electron lines in Sample 3 (1% H_2) where they strongly overlapped and nearly merged into a single broad structure (Fig. 4). The splitting between two electron lines in this sample was conspicuously smaller than in "pure" Ne Sample 1 (Fig. 3) and amounted to 2.5 G. We also clarified that the position of the e-H_2 component did not change from sample to sample, while the e-Ne line shifted toward smaller resonant magnetic fields (higher electronic g-factors) upon raising H_2 content in Ne from 100 ppm to 1% (Samples 1–3) where it was observed.

It turned out that the number of electrons trapped in the neon environment was nearly independent of the H_2 concentration for Samples 1–3 (100 ppm, 0.2 and 1% H_2) where this line was observed, while the number of electrons trapped in the H_2 environment increased in the samples with higher H_2 admixtures (Samples 4–6) and reached a maximum for Sample 5 (6% H_2). The areas of both electron lines in a steady state as functions of H_2 concentration are presented in Fig. 5. The equilibrium areas and widths of electron lines trapped in the pure Ne and H_2 environment for different samples are also summarized in Table 1.

3.2 Effect of Unsaturated Helium Film and Annealing

In our recent study of H atoms in solid Ne:H_2 mixtures [6], we found that raising temperature from 0.1 to 0.3–0.6 K and admitting a superfluid He film into the sample
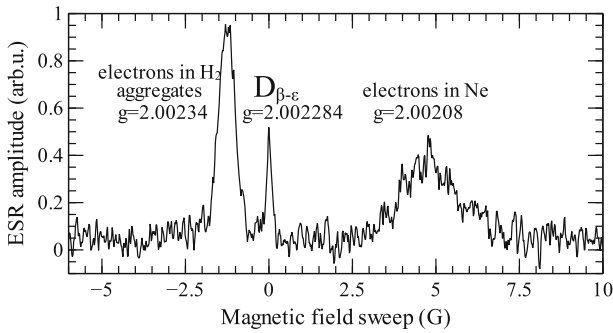
Fig. 3 Spectrum of electrons trapped in the "pure" Ne Sample 1 (100 ppm H_2) after condensing He film into sample cell. The $D_{\beta-\epsilon}$ line of deuterium atoms in the gas phase ($g = 2.002284$ [19]) was used as a reference
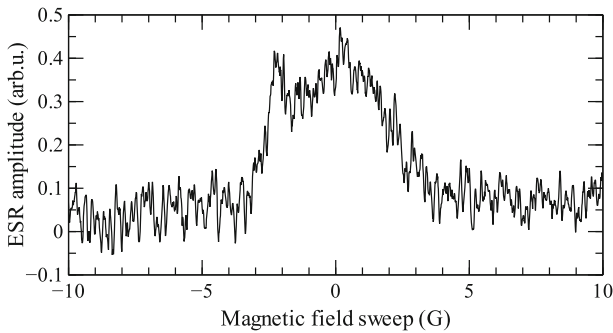

Fig. 4 The electron lines in the center of ESR spectrum of Ne:1% H_2 (Sample 3). Note that the splitting between two electron lines is smaller ($\simeq 2.5$ G) compared to that in Fig. 3. See Page 12 for detailed discussion
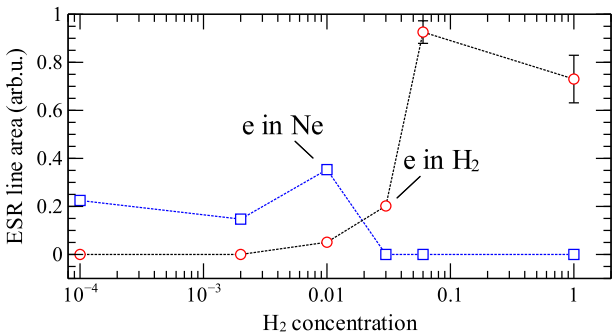

Fig. 5 Electron line areas as a function of the H_2 admixture in Ne:H_2 solids (red circles: in H_2 cluster, blue squares: pure Ne environment). The points for Samples 1–4 correspond to a saturation point when the electron line integrals stopped changing. The saturation points for Sample 5 (6% H_2) and pure H_2 Sample 6 were obtained by extrapolating the experimental data. The extrapolation errors for these two samples are shown as error bars (Color figure online)

Table 1 Characteristics of the samples studied in this work

Sample	1	2	3	4	5	6
[H_2] (%)	0.01	0.2	1	3	6	100
QM shift (Hz)	1450	–	–	1490	1130	10

Sample	Area (arb.u.)	Width (G)	He film	Annealing
e-H_2, narrow ESR line component				
1	–	–	Appeared	Disappeared
2	–	–	–	–
3	0.05	0.7	–	–
4	0.20	0.8	No effect	Decreased
5	0.93	0.7	No effect	Decreased
6	0.73	0.7	No effect	Decreased

Sample	Area (arb.u.)	Width (G)	He film	Annealing
e-Ne, broad ESR line component				
1	0.22	2.1	No effect	Disappeared
2	0.15	2.9	No effect	Disappeared
3	0.35	3.2	No effect	Disappeared
4	–	–	Absent	Absent
5	–	–	Absent	Absent
6	–	–	Absent	Absent

The areas and widths of the electron ESR signals are presented for as-prepared samples and were collected before condensing helium into the cell. The procedure of condensing He was not done for Samples 2 and 3. The QM shift is considered as the QM frequency change resulted from the adsorption of non-superfluid He layers on the surface of neon samples. The effects of condensing He film and annealing should be understood as following: "appeared": line area increased from zero to a certain value, "disappeared": line area decreased to zero, "absent": was not observed in this sample, "no effect": the action had no clear effect on the line area

cell triggered a nearly complete instantaneous recombination of H atoms trapped in H_2 clusters formed in solid neon and corresponding to Component 1 in Fig. 2. This effect turned out to be the most pronounced for the Ne:1% H_2 mixture sample. Based on that, we paid special attention to verify the effects of temperature and admission of the superfluid He film on the electron lines. In contrast to the loss of the Component 1 of the H atom signals (Fig. 2) observed in our previous work, raising temperature from 0.1 to 0.7–0.8 K did not influence either electron line.

At the next stage, we studied the influence of an unsaturated He film on the ESR spectra of electrons trapped in the Ne:H_2 samples. Condensing the helium film for Samples 1 also triggered the growth of the e-H_2 line (Fig. 3). The effect of condensing helium into the sample cell on different samples is summarized in Table 1.

We were also able to observe both electron lines after condensing an equal amount of ^{3}He into the cell while storing a "pure" Ne (100 ppm H_2) Sample 1. Based on that, we ruled out the possibility that this line may be related to ^{4}He$^+$ ions. The large
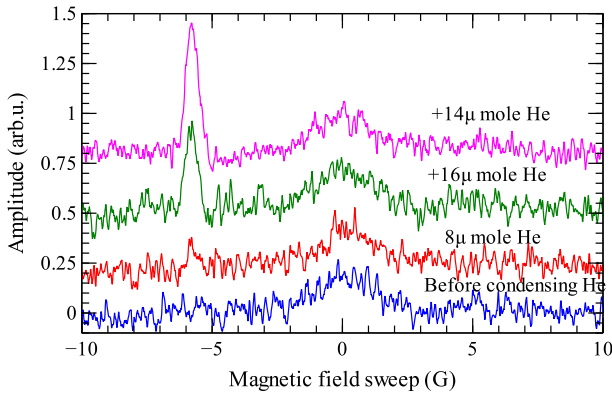
Fig. 6 ESR electron line evolution in "pure" Ne Sample 1 ($[H_2] = 100\,$ppm) during condensing He into the sample cell. The narrow line on the left is the e-H_2 line, which grows after condensing helium into the sample cell (Color figure online)

hyperfine interaction between the electron and nucleus for $^3He^+$ ions splits the ESR lines far aside from the central region [20].

We also observed that condensing a larger amount of helium into the sample cell resulted in an increase in the e-H_2 line (Fig. 6) while evacuating helium from the cell made it significantly smaller. We also tried to apply an electric potential to the floating top electrode of the QM in order to better understand the location of electrons which constitute the lines. Applying $\pm 80\,$V did not have any influence on the area or position of the e-H_2 nor for the broader line. Therefore, we suggest that the line accumulated after condensing the He film cannot be attributed to electrons on the surface of neon films which should be easily influenced even by a weak electric potential.

Condensing helium into the sample cell also resulted in a significant shift of the QM oscillation frequency, an effect which we employed to estimate the sample porosity. The QM is able to sense only the presence of non-superfluid He layers formed on its surface while the superfluid fraction is decoupled from the QM oscillations and cannot be detected. The frequency shifts after condensing He for as-deposited samples are large and summarized in Table 1.

We tried to estimate the porosity of the "pure" Ne sample by measuring the QM frequency shift upon condensing He film on top of the neon film. This study was carried out for a "pure" Ne ($100\,$ppm H_2) sample of the same thickness as Sample 1. We stabilized the sample cell temperature at $0.6\,$K and admitted He in small, $2\,\mu$mol, portions. The QM frequency change was carefully recorded after condensing each He portion (Fig. 7). The frequency shift appears to be larger for the first portions, while it decreases further from portion to portion when the superfluid He layers are formed. We were able to estimate the specific surface area, σ, of the as-deposited Ne sample by analyzing the QM frequency shifts after condensing He portions and comparing them to that induced by the deposition of the "pure" Ne film itself. The value found, $\sigma = 145\,m^2\,g^{-1}$, is smaller than that for zeolites (750–$1030\,m^2\,g^{-1}$), but approaches that of the nanocrystalline TiO_2 (160–$600\,m^2\,g^{-1}$) adsorbent.
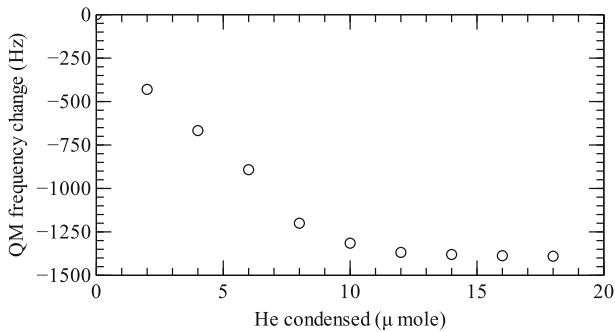
Fig. 7 The QM frequency shift as a function of amount of He gas condensed into the sample cell in 2 μmol portions during storage of a "pure" Ne sample

In addition, we also studied the influence of sample annealing on the ESR spectra of trapped electrons. The samples were annealed by raising the cell temperature to 7–10 K and for a time period of 1.5–2 h. Raising the temperature also resulted in a partial sample sublimation which was observed as an increase in the quartz microbalance operating frequency. Annealing typically resulted in a sublimation of $\simeq$ 10% of the sample mass. After that the sample cell was cooled to a temperature of 0.6 K and a small amount of a He gas was condensed into the sample cell in order to study the sample porosity. Condensing He into the cell in this case led to a frequency shift of about 300–400 Hz which provides evidence of a significant residual sample porosity. Annealing the samples with low H_2 concentrations, 100 ppm, 0.2% and 1% H_2 (Samples 1–3) destroyed the e-Ne line and Component 1 of ESR lines of H (Samples 1–3) corresponding to trapping of H atoms in H_2 clusters. In contrast, these lines survived annealing in samples containing higher, 3% and 6%, concentrations of H_2 (Sample 4, 5). Annealing Samples 4 and 5 had only a moderate effect on the e-H_2 line whose amplitude decreased by about 20%. The effect of annealing on different samples is summarized in Table 1.

4 Discussion

Several techniques were used previously for studies of ions and electrons in cryocrystals of hydrogen and its isotopes and rare-gas matrices, including infrared spectroscopy [21], ESR [18,22–24] registration of electron emission current [7] and detection of the cyclotron resonance of emitted electrons [4,25]. Ionization of matrix atoms or molecules was done by irradiation with UV, γ or x rays. This process was accompanied by rapid recombination of charged particles and various chemical tunneling reactions leading to a number of exotic ions stabilized in the solids [23,24,26]. In the other technique, the beams of electrons with energies of several keV and higher were directed on the solid samples [7,20]. A fraction of these electrons slowed down in the matrix and could thus be trapped there for sufficiently long time. Observation of free electrons in a pure hydrogen samples was difficult at temperatures above 2 K and required small admixtures of deuterium [22] which provides trapping sites for

electrons. In our previous work [18], we found that lowering the matrix temperature allows trapping free electrons even in pure H_2 matrices, but they start to escape from the matrix when its temperature is raised above $2\,K$. In these experiments, we performed accurate measurements of the g-factor and ESR line width for the trapped electrons, which helped to provide identification of spectral lines in the neon matrices presented in this report.

In the solid neon–hydrogen mixtures studied in this work, we observed two singlet ESR lines which we attribute to the trapped electrons, one broad (e-Ne) and one narrow (e-H_2). Position, shape and width of the narrow line well coincide well with the electron lines observed previously in pure hydrogen samples. This was also confirmed in a control experiment with the sample 6 of pure H_2 in this work. We assign the narrow line to the electrons trapped in the pure H_2 environment. The growth of this line in the samples 3–4 has saturated after several days of observations, whereas the accumulation of unpaired atoms in all samples continued with constant rates for much longer times. This implies a loss mechanism for the electrons which starts to work at substantially smaller densities than that for H atoms. This process cannot be a recombination with positive ions inside the matrix since our samples receive electrons from the metal walls of the sample cell. They cannot find excessive positive charge inside the films and must return back to the walls. Therefore, the diffusion of electrons toward the boundaries of the solid films, its lower and upper surfaces can be the only mechanism responsible for their loss.

Another observation made in this work is that the intensity of the e-H_2 line is strongly increased after admission of helium into the sample cell. In the samples 1 and 2 with small concentration of hydrogen, this line is not observed at all without admission of helium. This behavior can be explained by suppression of the loss mechanism of the trapped electrons due to the presence of liquid helium. Since we also see with QM measurements that helium penetrates into the pores of the neon film, it is natural to suggest that it blocks the channels connecting the pores and slows down diffusion of electrons from the bulk of the film. Pumping out helium partially opens the channels, but since it is not possible to completely remove the last one or two layers of helium, this partially opens channels and provides the escape channel for the electrons. Their density decreases, but remains larger than it was before admission of helium.

From our previous work [18] we learned that in pure hydrogen, diffusion of electrons toward the surfaces of hydrogen film is thermally activated and starts to work effectively only at temperatures above $2\,K$. Therefore, in order to explain why they diffuse below $1\,K$ in the neon matrices studied in this work, we suggest that substantial fraction of electrons is trapped close to the surface of hydrogen clusters located inside pores of solid neon. This fraction is larger for the samples with smaller concentration of hydrogen for which the effect of helium admission is strongest. For the samples 4–5 with highest concentration of hydrogen we did not observe a clear effect of helium on the intensity of the e-H_2 line. This can be explained by a larger size of the H_2 clusters and hence a larger fraction of electrons trapped in their bulk.

The influence of helium on the electron emission from the solid matrices of neon and hydrogen had been previously observed by several researchers. Leach [20] was able to detect electrons in solid hydrogen only after admission of superfluid helium, which he explained by the improvement in the thermal conductance of the samples. The

suppression of electron emission from solid neon upon condensing He was reported previously by Dmitriev [27,28]. Formation of a thin charged layer near the surface of rare-gas films exposed to an electron beam was discussed in Ref. [8], and it was concluded that the film surface can acquire a significant negative surface charge even after a very short exposure time. Accumulation of the sample charge discussed in Ref. [8] was also manifested by a smaller yield of secondary electrons which is reminiscent of the suppression of electron emission after condensing a He film observed in Refs. [27,28]. In all of the experiments mentioned above, the samples were quench condensed on much warmer substrates than in our case, and at much faster condensing rates. The porosity of such samples was not studied and could have been very large. Therefore, none of these observations contradict the above presented interpretation of our experimental results.

The high porosity and structural disorder is reminiscent of the impurity-helium condensates (IHC) which are formed by injecting a supersonic jet of impurity atoms and molecules into bulk superfluid helium [29]. The studies of H atoms stabilized in the Kr [30] and Ne [31] IHCs showed that some of H atoms prefer to accommodate in the H_2 layers formed at the rare-gas nanocluster surfaces, and they recombine upon annealing.

Based on the electronic g-factor, we assigned the second broad line to electrons stabilized in a pure Ne environment. The spin–orbit interaction with the neon atoms which possess p-electrons in their outer shells, slightly reduces the g-factor of electrons trapped in the neon environment compared to that for a free value. On the other hand, the absence of the spin–orbit interaction associated with H_2 molecules makes the g-factor of electrons trapped in H_2 clusters closely match the values for free electrons [32].

As a result of a small interatomic distance, $\simeq 3.1$ Å, a regular solid neon lattice cannot provide suitable sites for electrons and we suggest that electrons are preferentially trapped close to the pore surfaces where the neon lattice is highly disordered. It might be expected that the presence of a certain number of H_2 molecules in the closest neighborhood of trapped electrons in the predominantly Ne environment will shift their ESR lines toward smaller resonant magnetic fields (higher electronic g-factors). This was indeed observed in Samples 1 and 3 (100 ppm and 1% H_2) where the relative shift between two electron lines decreased from $\simeq 6$ to 2.5 G (Figs. 3, 4). A difference in the linewidth may be associated with an inhomogeneity of the trapping sites, leading to the g-factor spread for electrons in slightly different environments. Based on the QM frequency shifts after condensing He into the sample cell, it can be concluded that the pore surface area is similar for all as-deposited Ne:H_2 mixture samples. We suggest that the pore surfaces contain much smaller amounts of molecular hydrogen in the case of Samples 1–3 (100 ppm, 0.2% and 1% H_2, respectively), and the e-Ne ESR line could be observed because of its relatively small width. At higher concentrations of hydrogen in the samples, the surface coverage increases, and the line becomes too broad to be detected (samples 4–5).

Annealing Samples 1 and 2 with a small H_2 content, 100 ppm, 0.2% H_2, respectively, also resulted in a disappearance of the e-Ne line and the H atoms ESR line components corresponding to their stabilization in the H_2 clusters. It might be suggested that annealing Samples 1 and 2 led to formation of the equilibrium Ne:H_2 solid mixtures

which are characterized by the H_2 cluster dissolution and a more uniform distribution of H_2 molecules in the neon matrix.

5 Conclusions

We reported on the direct observation of electrons trapped in Ne:H_2 mixtures at $T <$ 1 K by means of electron spin resonance. Depending on the H_2 content, we observed two ESR lines in the center of ESR spectra which were attributed to electrons trapped in pure Ne and H_2 environments, respectively. We did not observe the ESR lines corresponding to trapping of electrons in the pure Ne environment in samples with the H_2 admixture exceeding 1%. We suggest that electrons are trapped preferentially close to the sample pore surface which become covered by molecular hydrogen in samples with higher H_2 content. Finally, we were able to estimate the specific surface of the as-deposited Ne films which turned out to be significant and nearly matching that of a nanocrystalline TiO_2 adsorbent.

References

1. V.E. Bondybey, A.M. Smith, J. Agreiter, Chem. Rev. **96**, 2113 (1996)
2. L. Andrews, M. Moskovits, *Chemistry and Physics of Matrix-Isolated Species* (North Holland, Amsterdam, 1989)
3. R. Clark, R. Hester, *Spectroscopy of Matrix Isolated Species* (Wiley, Chichester, 1989)
4. Y.A. Dmitriev, R.A. Zhytnikov, M. Kaimakov, Sov. J. Low Temp. Phys. **15**, 279 (1989)
5. T. Kiljunen, J. Eloranta, H. Kunttu, J. Chem. Phys. **110**(24), 11814 (1999)
6. S. Sheludiakov, J. Ahokas, J. Järvinen, L. Lehtonen, S. Vasiliev, Y.A. Dmitriev, D.M. Lee, V.V. Khmelenko, Phys. Rev. B **97**, 104108 (2018)
7. M. Frankowski, E.V. Savchenko, A.M. Smith-Gicklhorn, O.N. Grigorashchenko, G.B. Gumenchuk, V.E. Bondybey, J. Chem. Phys. **121**(3), 1474 (2004). https://doi.org/10.1063/1.1763568
8. Y. Bozhko, J. Barnard, N. Hilleret, arXiv:1302.2334v1 (2013)
9. K. Kajita, W. Sasaki, Surf. Sci. **113**(1), 419 (1982)
10. W. Schulze, D.M. Kolb, J. Chem. Soc. Faraday Trans. 2 Mol. Chem. Phys. **70**, 1098 (1974)
11. S.A. Nepijko, I. Rabin, W. Schulze, ChemPhysChem **6**(2), 235 (2005)
12. A.S. Barylnik, A.I. Prokhvatilov, M.A. Strzhemechny, G.N. Shcherbakov, Low Temp. Phys. **19**, 447 (1993)
13. N.N. Gal'tsov, A.I. Prokhvatilov, M.A. Strzhemechnyi, Low Temp. Phys. **30**(12), 984 (2004)
14. K. Kuyanov-Prozument, A.F. Vilesov, Phys. Rev. Lett. **101**, 205301 (2008)
15. S. Sheludiakov, J. Ahokas, O. Vainio, J. Järvinen, D. Zvezdov, S. Vasiliev, V.V. Khmelenko, S. Mao, D.M. Lee, Rev. Sci. Instrum. **85**(5), 053902 (2014)
16. S. Vasilyev, J. Jarvinen, E. Tjukanoff, A. Kharitonov, S. Jaakkola, Rev. Sci. Instrum. **75**(1), 94 (2004)
17. S. Sheludiakov, J. Ahokas, J. Järvinen, L. Lehtonen, O. Vainio, S. Vasiliev, D.M. Lee, V.V. Khmelenko, Phys. Chem. Chem. Phys. **19**, 2834 (2017)

18. S. Sheludiakov, J. Ahokas, J. Järvinen, O. Vainio, L. Lehtonen, D. Zvezdov, V. Khmelenko, D.M. Lee, S. Vasiliev, J. Low Temp. Phys. **183**(3), 120 (2015)

19. J. Vanier, C. Audonin, *The Quantum Physics of Atomic Frequency Standards*, vol. 1 (Adam Hilger, Bristol and Philadelphia, 1989), p. 24

20. R.K. Leach, A paramagnetic resonance study of hydrogen atom production and recombination in solid H_2 from 1.4 to 8 K. Ph.D. thesis, University of Wisconsin (1972)

21. J.A. Forrest, R.L. Brooks, J.L. Hunt, B. Stenum, J. Schou, H. Sorensen, P. Gürtler, F. Magnotta, E.R. Mapoles, P.C. Souers, G.W. Collins, Phys. Rev. B **46**, 13820 (1992)

22. G.W. Collins, P.C. Souers, F. Magnotta, E.R. Mapoles, J.R. Gaines, Phys. Rev. B **53**(13), 8143 (1996)

23. J. Kumagai, H. Inagaki, S. Kariya, T. Ushida, Y. Shimizu, T. Kumada, J. Chem. Phys. **127**(2), 024505 (2007)

24. M.D. Correnti, K.P. Dickert, M.A. Pittman, J.W. Felmly, J.J.I. Banisaukas, L.B. Knight Jr., J. Chem. Phys. **137**(20), 204308 (2012)

25. Y.A. Dmitriev, J. Low Temp. Phys. **180**(3), 284 (2015)

26. T. Miyazaki, K. Yamamoto, Y. Aratono, Chem. Phys. Lett. **232**(3), 229 (1995)

27. Y.A. Dmitriev, J. Low Temp. Phys. **150**(3), 544 (2008)

28. Y.A. Dmitriev, J. Low Temp. Phys. **158**(3), 502 (2009)

29. V.V. Khmelenko, H. Kunttu, D.M. Lee, J. Low Temp. Phys. **148**(1), 1 (2007)

30. R.E. Boltnev, E.P. Bernard, J. Järvinen, V.V. Khmelenko, D.M. Lee, Phys. Rev. B **79**, 180506 (2009)

31. S. Mao, A. Meraki, R.E. Boltnev, V.V. Khmelenko, D.M. Lee, Phys. Rev. B **89**, 144301 (2014)

32. F.J. Adrian, J. Chem. Phys. **32**(4), 972 (1960)